Geometry-induced charge separation on a helicoidal ribbon

Victor Atanasov*,†
Institute for Nuclear Research and Nuclear Energy, Bulgarian Academy of Sciences, 72 Tsarigradsko chaussee, 1784 Sofia, Bulgaria

Rossen Dandoloff‡
Department of Physics, CNRS-UMR8089, University of Cergy-Pontoise, F-95302 Cergy-Pontoise, France

Avadh Saxena§
Theoretical Division and Center for Nonlinear Studies, Los Alamos National Laboratory, Los Alamos, New Mexico 87545, USA
(Received 16 October 2008; published 12 January 2009)

We present an exact calculation of the effective geometry-induced quantum potential for a particle confined on a helicoidal ribbon. This potential leads to the appearance of localized states at the rim of the helicoid. In this geometry the twist of the ribbon plays the role of an effective transverse electric field on the surface and thus this is reminiscent of the Hall effect.

DOI: 10.1103/PhysRevB.79.033404 PACS number(s): 03.65.Ge, 73.43.Cd, 02.40.−k

The interplay of geometry and topology is a recurring theme in physics, particularly when these effects manifest themselves in unusual electronic and magnetic properties of materials. Specifically, helical ribbons provide a fertile playground for such effects. Both the helicoid (a minimal surface) and helical ribbons are ubiquitous in nature: they occur in biology, e.g., as beta sheets in protein structures,[1] macromolecules (such as DNA),[2] and tilted chiral lipid bilayers.[3] Many structural motifs of biomolecules result from helical arrangements:[4] cellulose fibrils in cell walls of plants, chitin in arthropod cuticles, and collagen protein in skeletal tissue. Condensed matter examples include screw dislocations in smectic A liquid crystals[5] and certain ferroelectric liquid crystals.[6] A helicoid to spiral ribbon transition[7] and geometrically induced bifurcations from the helicoid to the catenoid[8] have also been studied.

In this context, our goal is to answer the following questions: what kind of an effective quantum potential does a charge (or electron) experience on a helicoid or a helical ribbon due to its geometry (i.e., curvature and twist)? If the outer edge of the helicoid is charged, how is this potential modified and if there are any bound states? Our main findings are: the twist ω will push the electrons in vanishing angular-momentum state toward the inner edge of the ribbon and push the electrons in nonvanishing angular-momentum states to the outer edge, thus creating an inhomogeneous effective electric field between the inner and outer rims of the helicoidal ribbon. This is reminiscent of the Hall effect; only here it is geometrically induced. We expect our results to lead to new experiments on related twisted materials where the predicted effect can be verified. In a related context we note that de Gennes[9] had explained the buckling of a flat solid ribbon in terms of the ferroelectric polarization charges on the edges.

In order to answer the questions posed above, here we study the helicoidal surface to gain a broader understanding of the *interaction* between quantum particles and curvature, and the resulting possible physical effects. The properties of *free* electrons on this geometry have been considered before.[10] The results of this Brief Report are based on the Schrödinger equation for a confined quantum particle on a submanifold of $\mathbb{R}^3$. Following da Costa[11] an effective potential appears in the two-dimensional Schrödinger equation which has the following form:

$$V_{\text{curv}} = -\frac{\hbar^2}{2m^*}(M^2 - K), \tag{1}$$

where m^* is the effective mass of the particle, $\hbar$ is the Planck's constant, and M and K are the mean and the Gaussian curvature, respectively.

To describe the geometry we consider a strip whose inner and outer edges follow a helix around the x axis (see Fig. 1 with $\xi_0=0$). The surface represents a *helicoid* and is given by the following equation:

$$\vec{r} = x\vec{e}_x + \xi[\cos(\omega x)\vec{e}_y + \sin(\omega x)\vec{e}_z], \tag{2}$$

where $\omega=\frac{2\pi n}{L}$, L is the total length of the strip, and n is the number of 2π twists. Here $(\vec{e}_x,\vec{e}_y,\vec{e}_z)$ is the usual orthonor-

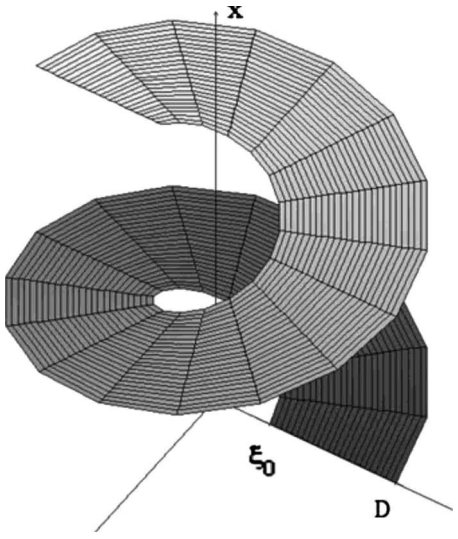

FIG. 1. A helicoidal ribbon with inner radius ξ_0 and outer radius D. For $\xi_0=0$ it becomes a helicoid. Vertical axis is along x and the transverse direction ξ is across the ribbon.

mal triad in $\mathbb{R}^3$ and $\xi \in [0,D]$, where D is the width of the strip. Let $d\vec{r}$ be the line element and the metric is encoded in

$$|d\vec{r}|^2 = (1+\omega^2\xi^2)dx^2 + d\xi^2 = h_1^2 dx^2 + h_2^2 d\xi^2,$$

where $h_1 = h_1(\xi) = \sqrt{1+\omega^2\xi^2}$ and $h_2 = 1$ are the Lamé coefficients of the induced metric (from $\mathbb{R}^3$) on the strip. Here is an appropriate place to add a comment on the *helicoidal ribbon*, which is a strip defined for $\xi \in [\xi_0, D]$ (see Fig. 1). All the conclusions still hold true and all of the results can be translated using the change in variables

$$\xi = \xi_0 + s(D-\xi_0), \quad s \in [0,1].$$

Here s is a dimensionless variable and one easily sees that for $\xi_0 \to 0$ we again obtain the helicoid.

The Hamiltonian for a quantum particle confined on the ribbon is given by

$$H = -\frac{\hbar^2}{2m^*}\frac{1}{h_1}\left[\left(\frac{\partial}{\partial\xi}h_1\frac{\partial}{\partial\xi}\right) + \frac{\partial}{\partial x}\frac{1}{h_1}\frac{\partial}{\partial x}\right] + V_{\text{curv}}. \tag{3}$$

Let us elaborate on the curvature-induced potential V_{curv}. Since the helicoid is a minimal surface, M vanishes and we are left with the following expression:

$$V_{\text{curv}} = \frac{\hbar^2}{2m^*}K = -\frac{\hbar^2}{2m^*}\frac{\omega^2}{[1+\omega^2\xi^2]^2}. \tag{4}$$

Using Gauss' *Theorema egregium*[12] the above potential can also be rewritten as

$$V_{\text{curv}} = \frac{\hbar^2}{2m^*}K = -\frac{\hbar^2}{2m^*}\frac{1}{h_1}\left(\frac{\partial^2 h_1}{\partial\xi^2}\right). \tag{5}$$

After rescaling the wave function $\psi \mapsto \frac{1}{\sqrt{h_1}}\psi$ (because we require the wave function to be normalized with respect to the area element $dxd\xi$), we arrive at the following expression for the Hamiltonian:

$$H = -\frac{\hbar^2}{2m^*}\left(\frac{\partial^2}{\partial\xi^2} + \frac{1}{h_1^2}\frac{\partial^2}{\partial x^2}\right) + V_{\text{eff}}(\xi), \tag{6}$$

where the effective potential in the (transverse) ξ direction is given by

$$V_{\text{eff}}(\xi) = -\frac{\hbar^2}{2m^*}\left[\frac{1}{2h_1}\left(\frac{\partial^2 h_1}{\partial\xi^2}\right) + \frac{1}{4}\frac{1}{h_1^2}\left(\frac{\partial h_1}{\partial\xi}\right)^2\right]. \tag{7}$$

Note that in bent tubular waveguides[13] and curved quantum strip waveguides[14] the effective potential is longitudinal. In the present case there is no longitudinal effective potential. After insertion of $h_1 = \sqrt{1+\omega^2\xi^2}$ the effective potential becomes

$$V_{\text{eff}}(\xi) = -\frac{\hbar^2}{4m^*}\frac{\omega^2}{(1+\omega^2\xi^2)^2}\left[1 + \frac{\omega^2\xi^2}{2}\right]. \tag{8}$$

This effective potential is of pure quantum-mechanical origin because it is proportional to $\hbar$. Note that this expression is exact and is valid not just for small ξ: here no expansion in a small parameter has been used.

Next, we write the time-independent Schrödinger equation as

$$\left[-\frac{\hbar^2}{2m^*}\frac{\partial^2}{\partial\xi^2} + V_{\text{eff}}(\xi)\right]\psi - \frac{\hbar^2}{2m^*}\frac{1}{h_1^2}\frac{\partial^2\psi}{\partial x^2} = E\psi. \tag{9}$$

Using the ansatz: $\psi(x,\xi) = \phi(x)f(\xi)$, we split the dependence on the variables and we get two differential equations:

$$-\frac{\hbar^2}{2m^*}\frac{d^2\phi(x)}{dx^2} = E_0\phi(x), \tag{10}$$

and

$$-\frac{\hbar^2}{2m^*}\frac{d^2 f(\xi)}{d\xi^2} + U(\xi)f(\xi) = Ef(\xi), \tag{11}$$

where

$$U(\xi) = V_{\text{eff}}(\xi) + \frac{E_0}{h_1^2(\xi)}. \tag{12}$$

With a solution $\phi(x) = e^{ik_x x}$ of Eq. (10) we have

$$E_0 = \frac{\hbar^2}{2m^*}k_x^2,$$

where k_x is the partial momentum in x direction. Let us consider here the azimuthal angle around the x axis: ωx and the angular momentum along this axis: $L_x = -\frac{i\hbar}{\omega}\frac{\partial}{\partial x}$. This operator has the same eigenfunctions $L_x\phi(x) = \hbar m\phi(x)$ as the operator in Eq. (10). The corresponding eigenvalues are $\hbar m$. We conclude that the momentum k_x is quantized

$$k_x = m\omega, \quad m \in \mathbb{N}.$$

This is not surprising because of the periodicity of the wave function along x. Note that the value of the angular-momentum quantum number determines the direction the electron takes along the x axis: either upward $m > 0$ or downward $m < 0$. This situation is reversed for a helicoid with opposite chirality.

Equation (11) represents the motion in the direction ξ with a net potential

$$U(\xi) = -\frac{\hbar^2}{2m^*}\frac{\omega^2}{4}\left\{\frac{1-4m^2}{(1+\omega^2\xi^2)} + \frac{1}{(1+\omega^2\xi^2)^2}\right\}, \tag{13}$$

which is depicted in Fig. 2.

This potential is a sum of two contributions: an attractive part $\frac{1}{(1+\omega^2\xi^2)^2}$ and a variable part which is repulsive for $|m| \geq 1$ and attractive for $m=0$ (see Fig. 2). The action of this part for $m \neq 0$ qualifies it as a centrifugal potential. It pushes a particle to the boundary of the strip. The finite size of the width D determines the cutoff of $U(\xi)$ and hence the probability of finding the particle is greatest near the rim of the helicoid. Since the behavior of the potential $U(\xi)$ for a particle with $m=0$ qualifies it as a quantum anticentrifugal one, it concentrates the electrons around the central axis for a helicoid (or the inner rim for a helicoidal ribbon). Such anticentrifugal quantum potentials have been considered before.[15]

The behavior described above can be inferred using the uncertainty principle. Localized states must appear away from the central axis or the inner rim. Physically, one may understand the appearance of localized states away from the

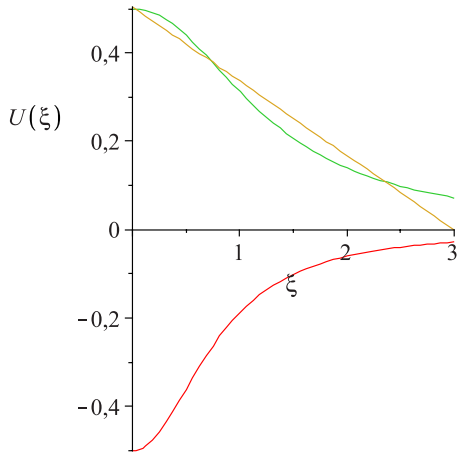

FIG. 2. (Color online) The behavior of the potential $U(\xi)$ for $\omega=1$ and $\hbar^2=2m^*=1$. Here the low-lying (red) curve corresponds to $m=0$, the upper-lying (green) curve to $m=1$, and the straight (yellow) line to the approximation given by Eq. (14).

central axis using the following reasoning: for larger ξ a particle on the strip will avail more space along the corresponding helix, and therefore the corresponding momentum, and hence the energy will be smaller than for a particle closer to the central axis.

We note that the separability of the quantum dynamics along x and ξ directions with different potentials points to the existence of an effective-mass anisotropy on the helicoidal surface. For the sake of simplicity let us approximate the potential $U(\xi)$ given in Eq. (13) (for $m=1$) by a straight line. The sole purpose of this approximation is to pinpoint the basic distribution of the probability density. Assuming it to be linear (see Fig. 2) and starting from certain $\xi_0=a\ll 1$,

$$U_a(\xi)=(D-\xi)\frac{U_0}{D-a},\quad U_0=U(\xi=a). \tag{14}$$

The value of a can be determined from an area preserving condition $\frac{1}{2}U_0(D-a)=\int_{\xi_0}^{D}U(x)dx$, where $\xi_0<D$ is the position from which we evolve the surface. When dealing with a helicoidal ribbon we must take $\xi_0\neq 0$. After obtaining a result for this case we can easily obtain a result for the helicoid case by taking the limit $\xi_0\to 0$.

Next we introduce a characteristic length scale l in the problem

$$l^{-3}=\frac{2m^*|U_0|}{\hbar^2(D-a)},\quad \frac{\lambda}{l^2}=\frac{2m^*}{\hbar^2}\left(E-\frac{DU_0}{D-a}\right),$$

where λ is a dimensionless energy scale. After introducing the dimensionless variable $\zeta=-\lambda-\xi/l$, the Schrödinger equation for the radial part becomes

$$\frac{d^2f}{d\zeta^2}-\zeta f(\zeta)=0, \tag{15}$$

with the following boundary conditions: $f(-\lambda-\xi_0/l)=f(-\lambda-D/l)=0$. This form of the equation is valid for $U_0>0$ as is the case for $m\neq 0$.

For $m=0$ we have a negative $U_0=-|U_0|$ which requires the introduction of the dimensionless variable $\zeta=-\lambda+\xi/l$ and the corresponding equation is given by Eq. (15), only in this case the boundary conditions are $f(-\lambda+\xi_0/l)=f(-\lambda+D/l)=0$. Let us assume that the ratio $D/l\gg 1$, then the solutions, i.e., the wave functions, of Eq. (15) coincide with the Airy function, that is, $f(\zeta)=\text{const}\,\text{Ai}(\zeta)$. Moreover the boundary condition $f(-\lambda\pm\xi_0/l)=0$ (the upper sign corresponds to $m=0$ and the lower to $m\neq 0$ states) gives the quantized energies

$$E_n(m)=U_0(m)\frac{D}{D-a}+\left(\lambda_n\pm\frac{\xi_0}{l}\right)\frac{\hbar^2}{2m^*l^2},$$

where λ_n are the zeroes of the Airy function $\text{Ai}(-\lambda_n)=0$. Let us list the first three of them: $(\lambda_1,\lambda_2,\lambda_3)=(2.338,4.088,5.521)$. Here we have taken account of the case when the interior of the helicoid is cut at a distance ξ_0 from the axis, which is the ribbon case. The helicoid case is obtained after setting $\xi_0\to 0$.

For the *vanishing angular-momentum state* we have $U_0(0)<0$ and the energy spectrum starts at a negative value (Fig. 2), that is, we have a *bound state*. The probability amplitude has a node at ξ_0 in the ribbon case or at the origin for the helicoid case. The evolution along ξ starts at the corresponding zero of the Airy function and evolves in the positive direction where the Airy function vanishes. For nonvanishing angular-momentum states we have $U_0(m)>0$ and the energy spectrum is positively valued (Fig. 2). The evolution of the corresponding solutions along ξ starts at the corresponding zero of the Airy function and evolves in the negative direction where the Airy function is oscillatory, as one would expect for a confined positive-energy spectrum. The observation that the $m\neq 0$ states at $\xi_0=\lambda_n l$ have the same energy $E_n(m)=U_0(m)D/(D-a)$ for all n leads us to believe that this is a particular positive-energy oscillatory state whose wavelength fits $D(1-\xi_0/l)\approx D(l/D\gg 1)$.

We would like to conclude with the observation that the electric-dipole moment for the $(m=0,\lambda_1)$ bound state (also the ground state for this geometrical configuration) is nonzero due to the anisotropic distribution of the probability density along ξ. Indeed, suppose we consider a ribbon doped with a uniform surface charge density σ, then the electric-dipole vector $\vec{p}=p_x\vec{e}_x+p_\xi\vec{e}_\xi$ in the moving coordinate system $(\vec{e}_x,\vec{e}_\xi,\vec{e}_3=\vec{e}_x\times\vec{e}_\xi)$ will have nonvanishing x and ξ components:

$$p_x=\frac{Q\pi}{\omega},\quad p_\xi=\frac{2\pi}{\omega}\sigma l^2\beta_n, \tag{16}$$

where the total charge is

$$Q=\int_0^{2\pi/\omega}dx'\int_{\xi_0}^{D}\sigma|\psi(x',\xi')|^2d\xi'$$

and

TABLE I. The values of β_n are summarized in the table.

	$n=1$	$n=2$	$n=3$	$n=10$
$m=0$	0.816	1.822	2.829	3.605
$m\neq 0$	2.712	2.451	2.299	1.783

$$\beta_n = \int_{\xi_0/l}^{D/l\gg 1} \left| \mathrm{Ai}\left(-\lambda_n \mp \frac{\xi_0}{l} \pm t \right) \right|^2 tdt.$$

Here the upper sign corresponds to $m=0$ and the lower to $m\neq 0$ states. For $\xi_0/l=0.1$ and $D/l=10$ we summarize the values of β_n in Table I.

Let us suppose that the outer rim of the helicoid is uniformly charged or there is a uniformly charged wire going through the core, then this will create an accelerating electric-field term in the effective potential $U(\xi)$, that is, $U^e(\xi)=U(\xi)+e\mathcal{E}\xi$. The dynamics is still separable. In the cup-shaped potential U^e the electrons will be found with the greatest probability where the potential has a minimum. This means that the extra charge on the helicoid will concentrate in a strip around the value of $\xi_{\min}$, i.e., a solution to $dU^e/d\xi=-e\mathcal{E}$.

Application of an electric or magnetic field along the x axis would nontrivially affect the motion of electrons on the surface. This problem will need to be studied numerically. Presently, we do not discuss any discreteness effects due to the underlying lattice structure of the material. Their inclusion can modify our findings qualitatively especially for materials whose band structure is not parabolic, e.g., graphene ribbons. Let us briefly discuss graphene whose low energy quasiparticles are described by the Dirac equation, not the Schrödinger equation studied here. Twisting a strip made out of graphene will stretch the carbon bonds and break the crystal rotational symmetry. Thus a geometry-dependent gap in the energy spectrum can be opened. We will address these interesting effects in a separate study.

For narrow strips the electron correlation effects are likely to be important. We consider the Thomas-Fermi-Weizsacker kinetic-energy functional versus the effective potential $U(\xi)$:

$$\frac{E_{\mathrm{TFW}}}{U(\xi\ll 1)} \approx \frac{1}{\omega^2}\int \frac{|\nabla n(\vec{r})|^2}{n(\vec{r})} d^2r,$$

where $n(\vec{r})$ represents the two-dimensional electron density. For materials where the geometry-dependent constraint $\int \frac{|\nabla n(\vec{r})|^2}{n(\vec{r})} dr < \omega^2$ holds true, we do not expect any qualitative change in our conclusions.

Our main findings can be summarized as follows: the twist ω will push the electrons with $m\neq 0$ ($m=0$) toward the outer (inner) edge of the ribbon, and create an effective electric field between the central axis and the helix, the latter representing the rim of the helicoids. Instead of a helicoidal ribbon, if we consider a cylindrical helical ribbon then both the curvature and torsion are constant and the effective potential is quite simple. We expect our results to motivate new low temperature ($T<\hbar^2/k_B 2m^* l^2$, where k_B is the Boltzmann constant) experiments on twisted materials.

This work was supported in part by the U.S. Department of Energy.

*Also at Department of Physics, CNRS-UMR8089, University of Cergy-Pontoise, F-95302 Cergy-Pontoise, France.
†victor.atanasov@u-cergy.fr
‡rossan.dandoloff@u-cergy.fr
§avadh@lanl.gov

[1] C. W. G. Fishwick, A. J. Beevers, L. M. Carrick, C. D. Whitehouse, A. Aggeli, and N. Boden, Nano Lett. **3**, 1475 (2003).
[2] J. Crusats *et al.*, Chem. Commun. (Cambridge) **13**, 1588 (2003).
[3] Ou-Yang Zhong-can and Liu Ji-xing, Phys. Rev. Lett. **65**, 1679 (1990); Phys. Rev. A **43**, 6826 (1991).
[4] J. M. Garcia Ruiz, A. Carnerup, A. G. Christy, N. J. Welham, and S. T. Hyde, Astrobiology **2**, 353 (2002).
[5] R. D. Kamien and T. C. Lubensky, Phys. Rev. Lett. **82**, 2892 (1999).
[6] D. M. Walba, E. Körblova, R. Shao, J. E. Maclennan, D. R. Link, M. A. Glaser, and N. A. Clark, Science **288**, 2181 (2000).
[7] R. Ghafouri and R. Bruinsma, Phys. Rev. Lett. **94**, 138101 (2005).
[8] A. Boudaoud, P. Patricio, and M. Ben Amar, Phys. Rev. Lett. **83**, 3836 (1999).
[9] P.-G. de Gennes, C. R. Acad. Sci., Ser. II: Mec., Phys., Chim., Sci. Terre Univers **304**, 259 (1987).
[10] R. Dandoloff and T. T. Truong, Phys. Lett. A **325**, 233 (2004).
[11] R. C. T. da Costa, Phys. Rev. A **23**, 1982 (1981).
[12] M. Spivak, *A Comprehensive Introduction to Differential Geometry* (Publish or Perish, Boston, 1999).
[13] J. Goldstone and R. L. Jaffe, Phys. Rev. B **45**, 14100 (1992).
[14] I. J. Clark and A. J. Bracken, J. Phys. A **29**, 339 (1996); **31**, 2103 (1998).
[15] M. A. Cirone, K. Rzazewski, W. P. Schleich, F. Straub, and J. A. Wheeler, Phys. Rev. A **65**, 022101 (2001); V. Atanasov and R. Dandoloff, Phys. Lett. A **371**, 118 (2007).